Applied Mathematics & Information Sciences
An International Journal

http://dx.doi.org/10.12785/amis/090520

Symbolic Dynamics and Big Bang Bifurcation in Weibull-Gompertz-Fréchet's Growth Models

J. Leonel Rocha[1,*], *Abdel-Kaddous Taha*[2] *and Danièle Fournier-Prunaret*[3]

[1] Instituto Superior de Engenharia de Lisboa-ISEL, ADM and CEAUL, Rua Conselheiro Emídio Navarro 1, 1959-007 Lisboa, Portugal
[2] NSA, University of Toulouse, 135 Avenue du Rangueil, 31077 Toulouse, France
[3] LAAS-CNRS, INSA, University of Toulouse, 7 Avenue du Colonel Roche, 31077 Toulouse, France

Received: 21 Jan. 2015, Revised: 22 Apr. 2015, Accepted: 23 Apr. 2015
Published online: 1 Sep. 2015

Abstract: In this paper, motivated by the interest and relevance of the study of tumor growth models, a central point of our investigation is the study of the chaotic dynamics and the bifurcation structure of Weibull-Gompertz-Fréchet's functions: a class of continuous-defined one-dimensional maps. Using symbolic dynamics techniques and iteration theory, we established that depending on the properties of this class of functions in a neighborhood of a bifurcation point P_{BB}, in a two-dimensional parameter space, there exists an order regarding how the infinite number of periodic orbits are born: the Sharkovsky ordering. Consequently, the corresponding symbolic sequences follow the usual unimodal kneading sequences in the topological ordered tree. We verified that under some sufficient conditions, Weibull-Gompertz-Fréchet's functions have a particular bifurcation structure: a big bang bifurcation point P_{BB}. This fractal bifurcations structure is of the so-called "box-within-a-box" type, associated to a boxe Ω_1, where an infinite number of bifurcation curves issues from. This analysis is done making use of fold and flip bifurcation curves and symbolic dynamics techniques. The present paper is an original contribution in the framework of the big bang bifurcation analysis for continuous maps.

Keywords: Weibull-Gompertz-Fréchet's growth models, symbolic dynamics, kneading sequences, big bang bifurcation, fold and flip bifurcation curves

This paper is dedicated to the memory of Professor José Sousa Ramos.

1 Introduction, preliminaries and motivation

In the last decades, the study of growth models has been one of the research topics of greatest relevance. Classical growth models such as the logistic, exponential, Gompertz, Richards, Von Bertalanffy and Blumberg equations continue to be widely and frequently used with success to describe several demographic, economic, ecological, biological and medical processes. In addition to these types of models, we can consider all special cases of the generalized logistic model and also of the Tsoularis-Wallace-Schaefer model, among other models studied, see for example [13], [14], [29], [31], [36] and references therein. In particular, the Gompertzian growth model was initially introduced as an actuarial function for the study of aging processes. Nowadays, the Gompertz function is widely used in several studies. Its application is highlighted in gene expression, enzyme kinetics, oxygenation of hemoglobin, intensity of photosynthesis and in the growth of organisms, cells, organs, tissues, tumours or populations, among other topics of investigation, see for example [9], [10], [30], [34], [35] and [37].

In [24], Rocha *et al* present a new dynamical approach to Weibull-Gompertz-Fréchet's growth models, defined by ordinary differential equations, whose particular solutions are extreme value distributions of Weibull, Gompertz and Fréchet type. For more details in extreme value distribution see for example [20]. In that work, the difference equations correspondent to Weibull-Gompertz-Fréchet's growth models are interpreted as non-linear coupling of probabilities, which determine Frechetzian, Gompertzian and Weibullzian dynamics, respectively. We remark that the dynamical study of these growth laws, defined as a family of unimodal maps, depends on two biological parameters:

* Corresponding author e-mail: jrocha@adm.isel.pt

the intrinsic growth rate of the number of individuals or cells and the growth-retardation factor. This characterization reflects the natural history of the malignant tumour.

The growth models of Weibull type are defined by the next normalized differential equation,

$$\frac{df_N(t)}{dt} = c\ f_N(t)\ (-\ln f_N(t))^{1-\frac{1}{\alpha}}, \text{ with } 0<\frac{1}{\alpha}<1, \quad (1)$$

where $f_N(t)$ is the normalized number or size of the population at an arbitrary time $t > t_0$ and $t_0 > 0$ is an initial time. The parameter c is an intrinsic growth rate or a retardation factor and α is a shape parameter or a growth-retardation factor. This model has light left tail and finite right endpoint, see Fig.1(a). This ordinary differential equation has a particular real solution, for $c = 1$, which is defined by the Weibull$-\alpha$ extreme value distribution, i.e.,

$$f_N(t) = \begin{cases} e^{-(-t)^\alpha} & \text{if } t < 0 \\ 1 & \text{if } t \geq 0 \end{cases}.$$

On the other hand, in [24] are also studied growth models of Fréchet type, which are established by the normalized differential equation,

$$\frac{df_N(t)}{dt} = c\ f_N(t)\ (-\ln f_N(t))^{1+\frac{1}{\alpha}}, \text{ with } \frac{1}{\alpha}>0. \quad (2)$$

Laws in the extreme value Fréchet domain of attraction for maxima must have infinite right endpoint, and can be severely heavy-tailed. Its right tail is heavier than in the standard gaussian, which is in the Gumbel domain of attraction, see Fig.1(c). A particular real solution of Eq.(2), for $c = 1$, is given by the Fréchet$-\alpha$ extreme value distribution, i.e.,

$$f_N(t) = \begin{cases} 0 & \text{if } t \leq 0 \\ e^{-t^{-\alpha}} & \text{if } t > 0 \end{cases}.$$

In particular, when $\frac{1}{\alpha} \to 0^+$ in Eqs.(1) and (2) is obtained the Gompertz growth model. This model has been extensively studied and used for compare dynamics of tumour growth in several host organisms, see for example [9], [10], [30], [37] and references therein. The differential equations (1) and (2) can be considered as particular cases of the Hyper-Gompertz growth model, introduced by Turner *et al* in 1976, see [34] and [35]. These models are also seen as a generalization of ecological growth function, or simply generalized Gompertz function.

Presently, the study and treatment of tumors is one of the most current and worrying problems in biological and medical research. In fact, the disease of cancer continues to be the scourge of humanity; being a leading cause of early death, and resistant to therapies aimed at its eradication. In this work, motivated by the interest and relevance of the study of tumor growth models, we investigated the chaotic dynamics and the bifurcations structure of Weibull-Gompertz-Fréchet's growth models. The purpose of this paper is to present an original contribution within the framework of growth models, simultaneously using techniques of symbolic dynamics and bifurcations theory.

The plan of the work is as follows. In Sec.2 we consider Weibull-Gompertz-Fréchet's functions and study their dynamical behavior. These families of unimodal maps are proportional to the right hand side of Eqs.(1) and (2), as stated in [24]. In Lemma 1 are presented sufficient conditions for the occurrence of stability of the fixed point, period doubling, chaos, chaotic semistability and non admissibility of Weibull-Gompertz-Fréchet's dynamics, dependent on the variation of the intrinsic growth rate.

In Sec.3, using iteration theory and symbolic dynamics techniques, the complex dynamical behavior of these functions is developed and investigated. Such as in Sec.2, this different approach allowed us to identify several population dynamics regimes. This study is completely characterized by the symbolic sequences associated to the critical point itinerary. In Table 1 can be seen a topological order for several symbolic sequences and their corresponding topological entropies, depending on the variation of the growth-retardation factor and of the intrinsic growth rate. See Appendix for details on symbolic dynamics theory.

Sec.4 is devoted to the study of bifurcation structures of Weibull-Gompertz-Fréchet's functions, in the two-dimensional (α, r) parameter space. This analysis is done in Subsec.4.1, based on the configurations of the fold and flip bifurcation curves. In Subec.4.2 we provide and discuss conditions for the existence of a big bang bifurcation point for these families of continuous functions. Typically, the big bang bifurcations are studied in the context of piecewise-smooth discontinuous dynamics. Moreover, this big bang bifurcation point is associated to the "box-within-a-box" fractal bifurcations structure. However, the sufficient conditions required by Mira in [17] for the existence of "box-within-a-box" fractal bifurcations structure are not satisfied for Weibull-Gompertz-Fréchet's functions throughout a parameter region. For this reason we consider Conjecture 1 to prove Proposition 1. In addition to the results obtained by symbolic dynamics techniques in Sec.3, to support our study in Sec.4, we present fold and flip bifurcations curves and a numerical simulation of the bifurcation diagram associated. Finally, in Sec.5, we discuss our results and provide some relevant conclusions.

2 Dynamical approach to growth models of Weibull-Gompertz-Fréchet (WGF) type

The aim of this section is to study a dynamical approach to Weibull-Gompertz-Fréchet's growth models,

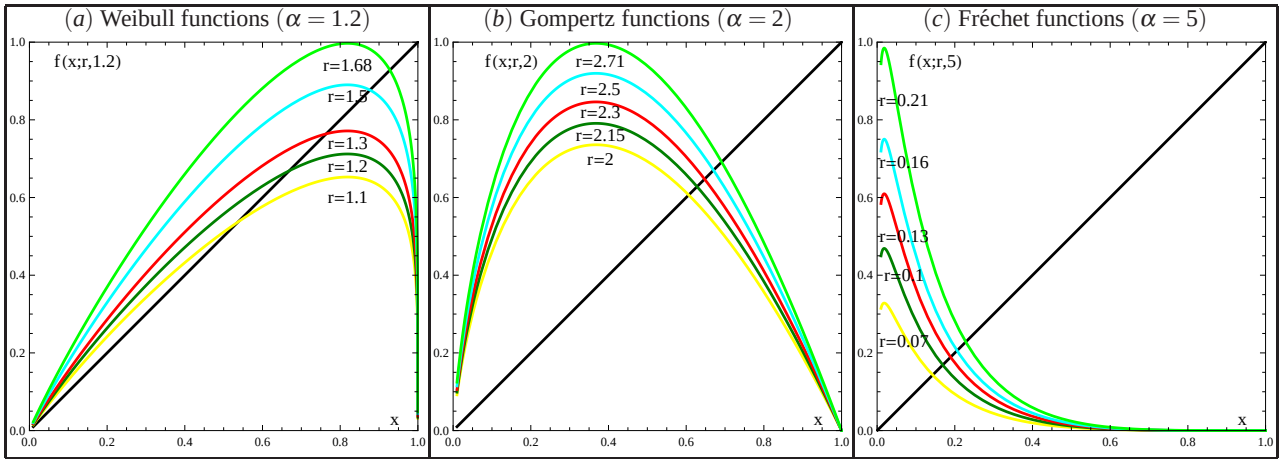

Fig. 1: Graphics of the Weibull-Gompertz-Fréchet's (WGF) functions $f(x;r,\alpha)$ for several parameters values of the intrinsic growth rate (r) and of the growth-retardation factor (α): Weibull functions at $\alpha = 1.2$ and $r = 1.1, 1.2, 1.3, 1.5, 1.68$; Gompertz functions at $\alpha = 2$ and $r = 2, 2.15, 2.3, 2.5, 2.71$ and Fréchet functions at $\alpha = 5$ and $r = 0.07, 0.1, 0.13, 0.16, 0.21$. Remark that some values of the intrinsic growth rates were chosen in order to illustrate the results presented in Table 1.

designated by Weibull-Gompertz-Fréchet's functions, which we will denote by WGF functions. This class of unimodal maps were firstly defined in [24]. Consider the family of functions $f :]0,1] \to [0,1]$, defined by

$$f(x;r,\alpha) = r\, x\, (-\ln x)^{\alpha-1} \tag{3}$$

where x is the normalized number of tumour cells or tumour size, $r > 0$ is an intrinsic growth rate of the number of cells (individual contribution), that summarizes mutual inhibitions between cells and the competition for nutrients, and it is sometimes viewed as a retardation factor, and $\alpha > 1$ is a shape parameter, that is sometimes called the growth-retardation factor. Considering the particular solutions of the differential equations given by Eqs.(1) and (2), we will say that: if $1 < \alpha < 2$, then $f(x;r,\alpha)$ are Weibull's functions; if $\alpha = 2$, then $f(x;r,\alpha)$ are Gompertz's functions; and if $\alpha > 2$, then $f(x;r,\alpha)$ are Fréchet's functions. We request claim particular attention to the diversity and complexity of these families of functions, which are exemplified in Fig.1.

The WGF functions satisfies the following conditions:

(A1) $f(x;r,\alpha)$ is continuous on $]0,1]$;
(A2) $f(x;r,\alpha)$ has a critical point $c \in]0,1[$, where $c = e^{1-\alpha}$;
(A3) $f'(x;r,\alpha) \neq 0, \forall x \in]0,1[\setminus\{c\}$, $f'(c;r,\alpha) = 0$ and $f''(c;r,\alpha) < 0$;
(A4) $f(x;r,\alpha) \in C^3(]0,1[)$;
(A5) the Schwarzian derivative of $f(x;r,\alpha)$ given by

$$S(f(x;r,\alpha)) = \frac{f'''(x;r,\alpha)}{f'(x;r,\alpha)} - \frac{3}{2}\left(\frac{f''(x;r,\alpha)}{f'(x;r,\alpha)}\right)^2,$$

verifies:

(i) $S(f(x;r,\alpha)) < 0, \forall x \in]x_1,x_2[\setminus\{c\}$, with
$S(f(x_1;r,\alpha)) = S(f(x_2;r,\alpha)) = 0,\ \forall 1 < \alpha < 2;$

(ii) $S(f(x;r,\alpha)) < 0, \forall x \in]x_1,1[\setminus\{c\}$, with
$S(f(x_1;r,\alpha)) = 0,\ \forall \alpha \geq 2.$

Remark that in condition (i) of $(A5)$ it is verified that $S(f(x;r,\alpha)) \geq 0,\ \forall x \in]0,x_1] \cup [x_2,1]$. This constraints cause problems that are analyzed in Sec.4. On the other hand, in condition (ii) of $(A5)$ it is verified that $S(f(x;r,\alpha)) \geq 0,\ \forall x \in]0,x_1]$. In this case, if we restrict the WGF functions to the interval

$$\left[x_1, max\{f^{-1}(y_1;r,\alpha)\}\right], \text{ with } y_1 = f(x_1;r,\alpha)$$

then this failure not disturb the dynamical behavior of this family of functions, as usual unimodal maps. The negative Schwarzian derivative ensures a "good" dynamic behavior of the models: continuity and monotonicity of topological entropy, order in the succession of bifurcations, the existence of an upper limit to the number of stable orbits and the non-existence of wandering intervals, [15] and [33]. See [32] to a topological dynamics approach of unimodal maps. The unimodal maps theory has proved to be useful in many branches of science. In population dynamics, aiming to model the growth of a certain species, the use of these families has been frequent. A similar approach is used at [1], [23], [24], [25], [26], [27] and [28].

We note that the WGF functions only have one fixed point, given by

$$A_{r,\alpha} = e^{-r^{(1-\alpha)^{-1}}}. \tag{4}$$

The existence of this unique fixed point implies that these growth models do not contemplate directly a region of extinction, because $x \in]0,1]$ and $x = 0$ is not a fixed point of the WGF functions f. However, this issue is debatable as we can see in [24], where is presented a regression or spontaneous extinction region that characterizes growth models of very small tumors, possibly unable to outwit immune surveillance.

The WGF functions also verify that,

$$\lim_{\alpha \to 1^+} f(x;r,\alpha) = rx. \tag{5}$$

In fact, when we consider the limit case $\alpha \to 1^+$, we have a degenerated case for this class of functions. This property will be the subject of study in Sec.4.

In the next result we provide sufficient conditions for the occurrence of stability, period doubling, chaos and non admissibility of WGF dynamics, dependent on the variation of the intrinsic growth rate r. This result is illustrated in Fig.2, at the (α, r) parameter plane.

Lemma 1. *Let $f(x;r,\alpha)$ be the WGF functions, defined by Eq.(3), with $r > 0$, $\alpha > 1$ and satisfying $(A1)-(A5)$. It is verified that:*

(i) (Stability region of $A_{r,\alpha}$) if $r < [2^{-1}(\alpha-1)]^{1-\alpha}$, then there is a linearly stable fixed point $A_{r,\alpha} \in]0,1[$ whose basin of attraction is $]0,1[$;

(ii) (Period doubling and chaotic regions) if $[2^{-1}(\alpha-1)]^{1-\alpha} < r < [e^{-1}(\alpha-1)]^{1-\alpha}$, then the interval $[f^2(c;r,\alpha), f(c;r,\alpha)]$ is forward invariant with basin of attraction $]0,1[$;

(iii) (Chaotic semistability curve) if $r = [e^{-1}(\alpha-1)]^{1-\alpha}$, then $]0,1]$ is invariant and verifies that

$$\bigcup_{n\geq 0} f^n(x;r,\alpha) = [0,1]$$

and

$$\lim_{n\to\infty} \frac{1}{n} |Df^n(x;r,\alpha)| > 0,$$

for Lebesgue almost every $x \in]0,1]$.

Proof. If $r < [2^{-1}(\alpha-1)]^{1-\alpha}$ and considering that by definition $r > 0$, Eq.(3), then $|f'(A_{r,\alpha};r,\alpha)| < 1$. Thus, the fixed point $A_{r,\alpha}$, given by Eq.(4), is linearly stable. By Modified Singer's Theorem, see [33], the point $A_{r,\alpha}$ is the only linearly stable fixed point in $]0,1[$ and the immediate basin of $A_{r,\alpha}$ includes the orbit of the critical point c. Thus, the interval $[c, f(c;r,\alpha)]$ is contained in the immediate basin of $A_{r,\alpha}$. As the point $A_{r,\alpha}$ is the only fixed point in $]0,1[$, this implies that $f(x;r,\alpha) > x$ on $]0,A_{r,\alpha}[$. Thus, the interval $]0, f(c;r,\alpha)]$ is also contained in the basin of attraction of $A_{r,\alpha}$. Considering that the WGF functions f map the interval $[f(c;r,\alpha),1[$ into $]0, f^2(c;r,\alpha)]$ and

$$]0, f^2(c;r,\alpha)] \subset]0, f(c;r,\alpha)[,$$

then $]0,1[$ is the basin of attraction of $A_{r,\alpha}$.

If $[2^{-1}(\alpha-1)]^{1-\alpha} < r < [e^{-1}(\alpha-1)]^{1-\alpha}$, then the fixed point $A_{r,\alpha}$ is not linearly stable. In this case, it is verified that $f(x;r,\alpha) > x$ on $x \in]0,c]$ and f has no fixed point at $]0,c]$. This implies that all the orbits of every $x \in]0,1[$ enters on the interval $[f^2(c;r,\alpha), f(c;r,\alpha)]$, after a finite time of iterations. As $f'(x;r,\alpha) < 0$ on $x \in]c,1]$, then f maps the interval $[c, f(c;r,\alpha)]$ into $[f^2(c;r,\alpha), f(c;r,\alpha)]$. On the other hand, considering that $f(x;r,\alpha) > x$ on $x \in]0,c]$, then f maps the interval $[f^2(c;r,\alpha), c]$ into $[f^2(c;r,\alpha), f(c;r,\alpha)]$. Thus,

$$f\left([f^2(c;r,\alpha), f(c;r,\alpha)]\right) \subseteq [f^2(c;r,\alpha), f(c;r,\alpha)],$$

i.e., the interval $[f^2(c;r,\alpha), f(c;r,\alpha)]$ is forward invariant with basin of attraction $]0,1[$.

Finally, if $r = [e^{-1}(\alpha-1)]^{1-\alpha}$, or in an equivalent way, $f(c;r,\alpha) = 1$, then there is an $r > 0$ such that the maximum size growth of the population is equal to the critical density. Clearly, the fixed point $A_{r,\alpha}$ is linearly unstable. Since it is verified that $f'(x;r,\alpha) > 0$ on $x \in]0,c[$, the WGF functions f maps $]0,c]$ into $]0, f(c;r,\alpha)]$. Also, since $f'(x;r,\alpha) < 0$ on $x \in]c, f(c;r,\alpha)]$ and $f(c;r,\alpha) = 1$, f maps $[c, f(c;r,\alpha)]$ into $[0,1]$. Hence, $]0,1]$ is invariant, which is called invariant absorbing segment of level one, see [18]. To show that this interval admits complex dynamics it suffices to check the conditions for which the WGF functions f on $]0,1]$ admits an ergodic absolutely continuous invariant measure, see the theorem presented in [19]. In fact, the WGF functions satisfy $(A1)-(A5)$ conditions. Also, it is verified that $f^2(c;r,\alpha) = 0$ and $f(0;r,\alpha)$ is not defined, then it follows that $f^n(c;r,\alpha)$ is not defined for $n > 2$. Thus, $f^n(c;r,\alpha) \neq c$, $\forall n > 2$. Considering that,

$$\lim_{x\to 0^+} f'(x;r,\alpha) > 1 \text{ and } f^2(c;r,\alpha) = 0,$$

the Modified Singer Theorem, [33], implies that the WGF functions on $]0,1]$ has no attracting periodic points. Thus, from the theorem presented by Misiurewicz in [19] and Birkhoff's Ergodic Theorem follows the properties of (iii).

We note that similar results to Lemma 1 are obtained to Blumberg's, Richards' and von Bertalanffy's growth models, in [26], [27] and [28], respectively.

Remark. Note that for WGF functions $f(x;r,\alpha)$, when r varies monotonically in the interval $]0,\bar{r}[$, where $\bar{r}$ is such that $f(c;\bar{r},\alpha) = 1$, there exist a fixed point $A_{r,\alpha}$ such that its multiplier ($\lambda = f'$ calculated at the fixed point) decreases monotonically from $+1$, and a fixed point with λ which increases monotonically from $+1$.

Fig.2 shows the bifurcation diagram of WGF functions $f(x;r,\alpha)$, at $(\alpha,r) \in]0,5]\times]0,3]$ parameter plane. The white region is the spontaneous extinction region, see Remark 3 of Sec.3. The blue region is the

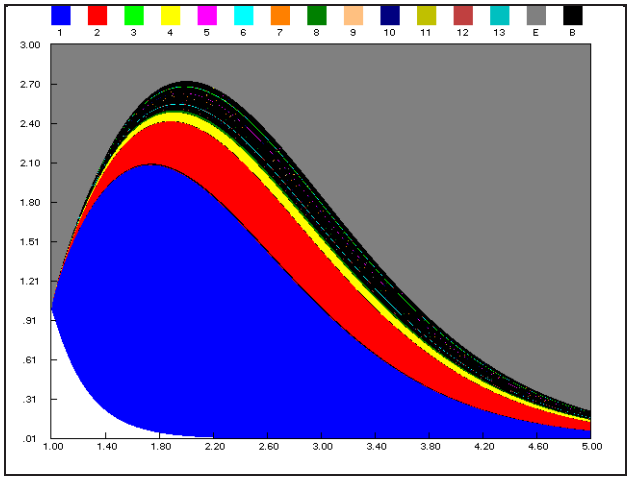

Fig. 2: Bifurcation diagram of WGF functions in the (α, r) parameter plane. The white region is the spontaneous extinction region, see Remark 3 of Sec.3. The blue region is the stability region. The region between the blue and the gray ones corresponds to period doubling region and chaotic region (existence region of cycles as shown on top of figure). The gray region is the non admissible region.

stability region of the fixed point $A_{r,\alpha}$, stated in Lemma 1 (i), that is upper bounded by the curve

$$\tilde{r}(\alpha) = [2^{-1}(\alpha-1)]^{1-\alpha}. \tag{6}$$

The region between the blue and the gray ones corresponds to period doubling region and chaotic region, also stated in Lemma 1 (ii). The period doubling region is well evidenced, highlighting in particular the cycles of order 2 and 4. The chaotic region is upper bounded by the curve

$$\bar{r}(\alpha) = [e^{-1}(\alpha-1)]^{1-\alpha}, \tag{7}$$

as stated in Lemma 1 (iii). This curve separates the chaotic region and the non admissible region; it is also designated by semi-stability curve, see also [31]. The gray region is the no admissible region. At this region the graphic of any WGF function is no longer totally in the invariant set $]0,1]$. Almost all trajectories of f (beasides a hyperbolic set of zero measure) leave the interval $]0,1]$ and either escape to infinity. The maps under these conditions are not good models for tumor or population dynamics. The curves $\tilde{r}(\alpha)$ and $\bar{r}(\alpha)$ are bifurcations curves and are studied in detail on Sec.4.

3 Symbolic Dynamics of WGF functions

This section is also devoted to the study of the dynamical behavior of the proposed models. However, this study is done based on symbolic dynamics techniques, see the Appendix for more details. The complexity of these models, described by the WGF functions, is displayed as a function at the (α, r) parameter plane. Different population dynamics regimes are identified, when the intrinsic growth rate r and the shape parameter or the growth-retardation phenomena α are modified. Generically, the dynamics of the WGF functions $f(x;r,\alpha)$, at the two-dimensional (α, r) parameter space, split in the following categories: stability, period doubling, chaos, chaotic semistability and non admissibility.

From the point of view of the population dynamics, a behavior of stability is defined when a population persists for intermediate initial densities and otherwise goes extinct. The *per capita* growth rate of the population is greater than one for a subinterval of population densities, see [23], [24], [25] and [31]. On the other hand, the symbolic dynamics techniques prove to be a good alternative to determine an approximation to the stability region. Generically, in the (α, r) parameter plane, the stability region is characterized by the iterates of the critical point that are always attracted to the positive fixed point $A_{r,\alpha}$, given by Eq.(4). The case where $A_{r,\alpha} \equiv c$ corresponds to the superstability, the point $A_{r,\alpha}$ is super stable or super attractive when it is merging with c. Thus, we have,

$$\lim_{n\to\infty} f^n(c;r,\alpha) = A_{r,\alpha}, \quad \text{for } 0 < r(\alpha) < \hat{r}(\alpha)$$

where $\hat{r}(\alpha)$ represents the super stable curve of the cycle of order 2, given in implicit form by $f^2(c;r,\alpha) = c$. Note that the curve $\hat{r}(\alpha)$ is distinct from the curve $\tilde{r}(\alpha)$, given by Eq.(6), as stated in Lemma 1 (i).

In the (α, r) parameter plane, the set of the super stable or super attractive points defines the super stable curves of the cycle of order $n = 1$. In the region before reaching the super stable curve, the symbolic sequences associated to the critical points orbits are of the type CL^{∞}. After this super stable curve, the symbolic sequences are of the type CR^{∞}, see Table 1. In this parameter region, the topological entropy of $f(x;r,\alpha)$ is null, see for example [12], [16], [24] and [25].

Remark. For some applications of these models, such as tumor growths, it is convenient to consider in the stability region a subregion designated by spontaneous extinction or tumour regression region, see [24]. This region is characterized by growths models of very small tumours, possibly unable to outwit immune surveillance. In this region, the iterates of the WGF functions $f(x;r,\alpha)$ are always attracted to a fixed point x_0 sufficiently close to zero, with $\alpha > 1$ and

$$0 < r(\alpha) < r_1(\alpha) = (-\ln(x_0))^{1-\alpha}.$$

In this context, the concept of the fixed point x_0 "sufficiently close to zero" must be related to the

Table 1: Topological order: symbolic sequences or kneading sequences associated to k–periodic orbit of the critical point c, the growth-retardation factor at $\alpha = 1.01, 1.02, 1.05, 1.1, 1.2, 1.6, 2, 3.5, 5$, and topological entropy ($h_{top}(f)$) for several values of the intrinsic growth rate (r). Figs.1 and 4 illustrate graphics of the WGF functions corresponding to some values considered in this table.

k	$S^{(r)}$	$\alpha = 1.01$	$\alpha = 1.02$	$\alpha = 1.05$	$\alpha = 1.1$	$\alpha = 1.2$	$\alpha = 1.6$	$\alpha = 2$	$\alpha = 3.5$	$\alpha = 5$	h_{top}
2	$(CR)^{\infty}$	1.05550	1.09875	1.20879	1.36334	1.61809	2.1914	2.2184	0.7417	0.0946	0.000
4	$(CRLR)^{\infty}$	1.05648	1.10079	1.21442	1.37606	1.64842	2.3170	2.4342	0.9355	0.1371	0.000
8	$(CRLR^3LR)^{\infty}$	1.05667	1.10119	1.21551	1.37853	1.65436	2.3421	2.4784	0.9786	0.1474	0.000
6	$(CRLR^3)^{\infty}$	1.05728	1.10169	1.21690	1.38168	1.66193	2.3744	2.5356	1.0360	0.1614	0.241
8	$(CRLR^5)^{\infty}$	1.05728	1.10194	1.21758	1.38323	1.66565	2.3904	2.5641	1.0654	0.1688	0.304
5	$(CRLR^2)^{\infty}$	1.05728	1.10245	1.21900	1.38646	1.67344	2.4241	2.6246	1.1294	0.1853	0.414
3	$(CRL)^{\infty}$	1.05747	1.10285	1.22011	1.38899	1.67956	2.4508	2.6730	1.1821	0.1994	0.481
6	$(CRL^2RL)^{\infty}$	1.05748	1.10288	1.22019	1.38916	1.67997	2.4526	2.6763	1.1858	0.2004	0.481
5	$(CRL^2R)^{\infty}$	1.05758	1.10308	1.22074	1.39042	1.68302	2.4660	2.7007	1.2130	0.2078	0.544
7	$(CRL^2R^3)^{\infty}$	1.05760	1.10323	1.22087	1.39071	1.68372	2.4691	2.7062	1.2192	0.2095	0.562
8	$(CRL^2R^2LR)^{\infty}$	1.05763	1.10317	1.22106	1.39114	1.68458	2.4728	2.7132	1.2270	0.2117	0.591
∞	CRL^{∞}	1.05765	1.10322	1.22114	1.39133	1.68520	2.4756	2.7182	1.2328	0.2133	$\ln 2$

specificity of the tumours growths investigation and clinical therapy. Thus, the spontaneous extinction region illustrated in Fig.2 is upper bounded by the curve $r_1(\alpha)$, considering $x_0 = 10^{-8}$. The symbolic sequences associated to the critical point orbits of these maps are of the type CL^{∞}, an aperiodic orbit, and its topological entropy keeps null. In Fig.4 are presented graphics of the WGF functions $f(x;r,\alpha)$ at $\alpha = 1.01$ and $r = 0.9$ and $r = 0.5$, which illustrate this special case.

The period doubling region corresponds to the parameters values in the (α, r) parameter plane, to which the population size oscillates asymptotically between 2^n states, with $n \in \mathbb{N}$. A cascade of sudden changes provokes the oscillation of the (two possible) values of population size in several limit cycles of period 2^n. In period doubling cascade, the symbolic sequences corresponding to the iterates of the critical point are determined by the iterations $f^{2^n}(c;r,\alpha) = c$, with c the critical point of $f(x;r,\alpha)$. Analytically, these equations define the super-stability curves of the cycle of order 2^n. In the (α, r) parameter plane, the period doubling region is bounded below by the curve of the intrinsic growth rate values where the period doubling starts, $\tilde{r}(\alpha)$, given by Eq.(6), correspondent to the 2-period symbolic sequences $(CR)^{\infty}$, see Table 1. Usually, the upper limit of this region is determined using values of intrinsic growth rate $r(\alpha)$, corresponding to the first symbolic sequence with non null topological entropy. Commonly, in the numerical results, the symbolic sequence that identifies the beginning of chaos is $\left(CRLR^3\right)^{\infty}$, a 6-periodic orbit, see Table 1, [24] and [25]. However, can be identified symbolic sequences whose period is less in Sharkovsky's ordering, see [32], for example the 10-periodic orbit $\left(CRLR^3LRLR\right)^{\infty}$. We remark that the symbolic dynamics techniques to determine this upper limit is an approximation as good as we want. The unimodal maps in this region also have null topological entropy, see for example [12], [16], [24] and [25].

In the chaotic region, the symbolic dynamics is characterized by iterates of the WGF functions $f(x;r,\alpha)$ that originate orbits of several types, which already present patterns of chaotic behavior, as stated in Lemma 1 (ii). In this region the topological entropy is a non-decreasing function related to the parameter r, until reaches the maximum value $\ln 2$, see [15]. This result is a consequence of the negative Schwartzian derivative and is observed for some parameter values in the last column of Table 1. In the (α, r) parameter plane, the chaotic region is bounded below by the curve of the intrinsic growth rate values where the chaos starts, as discussed in Sec.4. The upper limit is the curve of the intrinsic growth rate values for which the chaotic semi-stability curve appears.

In the chaotic semistability curve the dynamical behavior of the WGF functions $f(x;r,\alpha)$ is chaotic and this curve is defined by $f(c;r,\alpha) = 1$, given by Eq.(7) and stated in Lemma 1 (iii). The symbolic sequence associated to the chaotic semistability curve is of the type CRL^{∞}, with topological entropy $\ln 2$, see Table 1. After the chaotic region we have a non admissible region. In this case, there is no essential extinction region as in the cases of existence of Allee effect, see [23] and [26]. The non admissible region includes the values of the parameters for which the intrinsic growth rates $r(\alpha) > \overline{r}(\alpha)$, see Eq.(7) and Fig.2. The graphic of any WGF function is no longer totally in the invariant set $]0,1]$. The maps under these conditions not already belong to the studied families of the WGF functions and are not good models for populations dynamics.

Table 1 illustrate the application of the iteration theory and the symbolic dynamics techniques to the WGF functions. In this table can be seen a topological order for several symbolic sequences and their corresponding topological entropies, depending on the variation of the growth-retardation factor (α) and of the intrinsic growth

rate (r). From these numerical results, it was concluded that exists a monotonicity of the topological entropy and isentropic curves. This results are also verified in others growth models, see for example [24] and [25].

Remark. The numerical values obtained allow us to establish that when $\alpha \to 1^+$ it is verified that $r \to 1^+$. The symbolic sequences follow the usual unimodal kneading sequences in the topological ordered tree, see [11], [21] and [22]. Thus, depending on the properties of the WGF functions in a neighborhood of the point $(\alpha \to 1^+, r \to 1^+)$, which we will denote by P_{BB}, there exist an order regarding how the infinite number of periodic orbits are born: the Sharkovsky ordering, [32]. See [5] for the discontinuous case. On the other hand, the numerical results obtained via the symbolic dynamics are in agreement with the results given by Eq.(5). This special behavior in the neighborhood of the point P_{BB}, in the (α, r) parameter plane, is the motivation for the study presented in the next section: a global fractal bifurcation organization generated by the WGF functions.

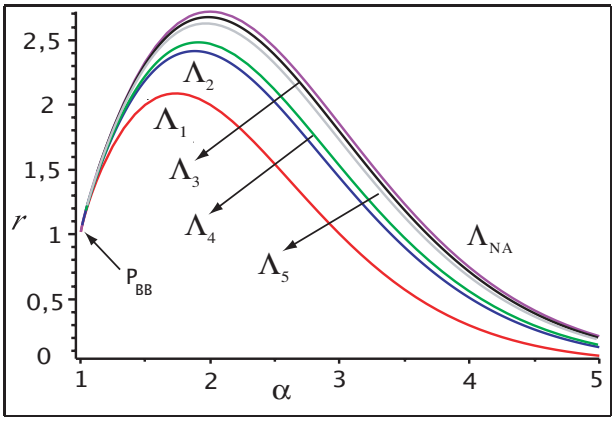

Fig. 3: Bifurcation curves of WGF functions in the (α, r) parameter plane. Λ_1, Λ_2, Λ_3, Λ_4 and Λ_5 are the flip bifurcation curves of the cycles of order $n = 1,2,3,4,5$, respectively; Λ_{NA} is the bifurcation curve of non admissibility (chaotic semistability curve) and P_{BB} is the big bang bifurcation point.

4 Bifurcation structures of WGF functions

The study of bifurcations is made to investigate behaviors of the system on the parameter plane in order to know which cycles are observed to the variation of parameters. In Subsec.4.1 we recall briefly some fundamental definitions in bifurcation theory, we will employ the classical fold and flip bifurcations. For more details on bifurcation theory see for example [7], [17] and [18]. In Subsec.4.2, another kind of bifurcation point is evidenced for WGF functions, in the two-dimensional (α, r) parameter space. This point is called big-bang bifurcation point and is associated with a particular bifurcation structure. Subsec.4.2 is devoted to the study of this special type of bifurcation, where we provide and discuss sufficient conditions for the existence of a big bang bifurcation point for WGF functions.

4.1 Fold and flip bifurcations of WGF functions

In this section we investigate in detail the bifurcation structure of the WGF functions, in the two-dimensional (α, r) parameter space. We say that an order n cycle $(x_1, x_2, ..., x_n)$ is stable (or attractive) iff

$$\left| \frac{\partial f^n}{\partial x}(x_j; r, \alpha) \right| < 1, \ \ \forall j = 1, 2, ..., n.$$

The *fold* bifurcation corresponds to the appearance of two order n cycles, one stable and the other unstable, when it is verified

$$\frac{\partial f^n}{\partial x}(x_j; r, \alpha) = 1, \ \ \forall j = 1, 2, ..., n.$$

On the other hand, the flip bifurcation corresponds to the change of stability of an order n cycle and the appearance of an order $2n$ cycle. Before the bifurcation, the order n cycle is stable, after the bifurcation, the order n cycle is unstable and the $2n$ cycle is stable. At the bifurcation it is verified that,

$$\frac{\partial f^n}{\partial x}(x_j; r, \alpha) = -1, \ \ \forall j = 1, 2, ..., n.$$

Generically, to WGF functions $f(x; r, \alpha)$, defined by Eq.(3), with $r > 0$ and $\alpha > 1$, the fold and flip bifurcation curves relative to a cycle of order n are determined as follows. If $x \in]0, 1[$ is a point of an order n cycle that satisfies the equations

$$f^n(x; r, \alpha) = x \ \text{ and } \ \frac{\partial f^n}{\partial x}(x; r, \alpha) = 1 \qquad (8)$$

then there exists a solution φ_n, such that the fold bifurcation curves relative to a cycle of order $n \in \mathbb{N}$ are given by $r = \varphi_n(x; \alpha)$, and are denoted by $\Lambda_{(n)_0}$. On the other hand, if $x \in]0, 1[$ is such that,

$$f^n(x; r, \alpha) = x \ \text{ and } \ \frac{\partial f^n}{\partial x}(x; r, \alpha) = -1 \qquad (9)$$

then exists a solution ψ_n, such that the flip bifurcation curves relative to a cycle of order $n \in \mathbb{N}$ are given by $r = \psi_n(x; \alpha)$, and are denoted by Λ_n, see some examples in Fig.3.

In particular, to WGF functions $f(x; r, \alpha)$, defined by Eq.(3), with $r > 0$ and $\alpha > 1$, the fold bifurcation curve of the fixed point $A_{r,\alpha}$, corresponding to Eq.(8) for $n = 1$,

has no meaning at the (α, r) parameter plane. Reason why for these models does not exist an extinction region. Note that the fold bifurcation curve $\Lambda_{(1)_0}$ is the bifurcation curve which defines the transition between the extinction region and the stability region, see also [23] and [26].

On the other hand, the flip bifurcation curve Λ_1 correspondent to Eq.(9) for $n = 1$, i.e., the flip bifurcation curve of the nonzero stable fixed point $A_{r,\alpha}$, is defined by

$$x = e^{-r^{(1-\alpha)^{-1}}} \quad \text{and} \quad \psi_1(x;\alpha) = [2^{-1}(\alpha-1)]^{1-\alpha}. \quad (10)$$

Note that the flip bifurcation curve Λ_1 is the bifurcation curve which defines the transition between the stability region and the period doubling region, such as established in Lemma 1 (i) and Eq.(6). In Fig.3 is presented in detail some flip bifurcation curves for the WGF functions.

So, the period doubling region is bounded below by the flip bifurcation curve Λ_1, of the stable fixed point $A_{r,\alpha}$. The upper limit of this region is defined by the accumulation value of the flip bifurcation curves of the cycle of order 2^n, of the stable fixed points nonzero, see [17] and [18]. This bifurcation curve is denoted by Λ_∞, from Eq.(9) and considering $x \in]0,1[$ a fixed point, we have,

$$\Lambda_\infty = \lim_{n\to\infty} \psi_{2^n}(x;\alpha).$$

The chaotic region is upper bounded by the chaotic semistability curve or fullshift curve, as stated in Lemma 1 (iii) and Eq.(7). This bifurcation curve is denoted by Λ_{NA} and is given by

$$\begin{aligned}\Lambda_{NA} &= \left\{(\alpha,r) \in \mathbb{R}^2 : f(c;r,\alpha) = 1\right\} \\ &= \left\{(\alpha,r) \in \mathbb{R}^2 : r = \zeta(\alpha), \zeta(\alpha) = [e^{-1}(\alpha-1)]^{1-\alpha}\right\}. \end{aligned} \quad (11)$$

Note that this curve defines the transition from the chaotic region to the non admissible region, see Fig.3.

In order to discuss the new kind of bifurcations for WGF functions, in the next section, the big bang bifurcation point in the (α, r) parameter plane, the following property is needed.

Property 1. Let $f(x;r,\alpha)$ be the WGF functions, defined by Eq.(3), with $\alpha > 1$, $r > 0$ and satisfying $(A1) - (A5)$, Λ_1 be the flip bifurcation curve for $n = 1$, given by $r = \psi_1(x;\alpha)$, Eq.(10), and Λ_{NA} be the semi-stability curve, given by $r = \zeta(\alpha)$, Eq.(11). In the limit case, when $\alpha \to 1^+$, it is verified that the flip bifurcation curve Λ_1 and the chaotic semi-stability curve Λ_{NA} converge to the bifurcation point $P_{BB} = (\alpha \to 1^+, r \to 1^+)$.

Proof. Considering the limit case, when $\alpha \to 1^+$ and $\forall r > 0$, in the equation that defines the chaotic semistability curve Λ_{NA}, given by Eq.(11), one has

$$\lim_{\alpha\to 1^+} \zeta(\alpha) = \lim_{\alpha\to 1^+} [e^{-1}(\alpha-1)]^{1-\alpha} = 1^+.$$

Thus, the convergence of the bifurcation curve Λ_{NA} to the bifurcation point $P_{BB} = (\alpha \to 1^+, r \to 1^+)$ follows.

On the other hand, given the flip bifurcation curve for $n = 1$, Eq.(10), considering $\alpha \to 1^+$ and $\forall r > 0$, the bifurcation curve Λ_1 verifies

$$\lim_{\alpha\to 1^+} \psi_1(x;\alpha) = \lim_{\alpha\to 1^+} [2^{-1}(\alpha-1)]^{1-\alpha} = 1^+,$$

and consequently, we obtain the following value for the respective fixed point

$$\lim_{r\to 1^+} \lim_{\alpha\to 1^+} e^{-r^{(1-\alpha)^{-1}}} = 1.$$

This means that, in this limit case, the flip bifurcation curve Λ_1 and the chaotic semi-stability curve Λ_{NA} intersect on the point $P_{BB} = (\alpha \to 1^+, r \to 1^+)$, as we wished to prove. See also Fig.3.

4.2 Big bang bifurcation of WGF functions

Big bang bifurcations occur typically in the context of piecewise-smooth discontinuous dynamics, whenever two fixed points cross simultaneously the boundary and become virtual. These kinds of bifurcation points are evidenced in the two-dimensional parameter space, characterizing particular regions always associated with cycles of different periods. At our knowledge, this bifurcation point was identified for the first time in [6], but the designation of "big bang"' was not given. In [2] it was proposed that these specific bifurcations be designated as big bang bifurcations. For more details about big bang bifurcations see for example [3], [4] [5], [8] and references therein. In the cited references it was shown that there are several types of big bang bifurcations, which cause different kinds of bifurcation scenarios. We remark that in [26] are given sufficient conditions for the occurrence of big bang bifurcations for a class of continuous maps: Blumberg's functions.

As previously indicated in Sec.2, the WGF functions $f(x;r,\alpha)$ satisfy the conditions $(A1) - (A5)$ and Remark 2. In particular, it is also verified that $f(x;r,\alpha)$ are continuous with respect to the parameter $r > 0$. However, as noted in (i) of $(A5)$, the Schwarzian derivative of the WGF functions is not negative throughout the interval $]0,1]$, for the parameters values $1 < \alpha < 2$. See some examples of graphics of the WGF functions $f(x;r,\alpha)$ under these conditions at Fig.4. As is known in other studies, this disturbance alters some of the classical properties in the behavior of bifurcations, see for example [26] and [32]. These special characteristics lead us to predict some changes in bifurcation structure of the WGF functions, restricted to the parameter region

$$R = \left\{(\alpha,r) \in \mathbf{R}^2 : 1 < \alpha < 2,\ r > 0\right\}.$$

Thus, the sufficient conditions required by Mira in [17] for the existence of "box-within-a-box" fractal bifurcations structure are not satisfied for WFG functions,

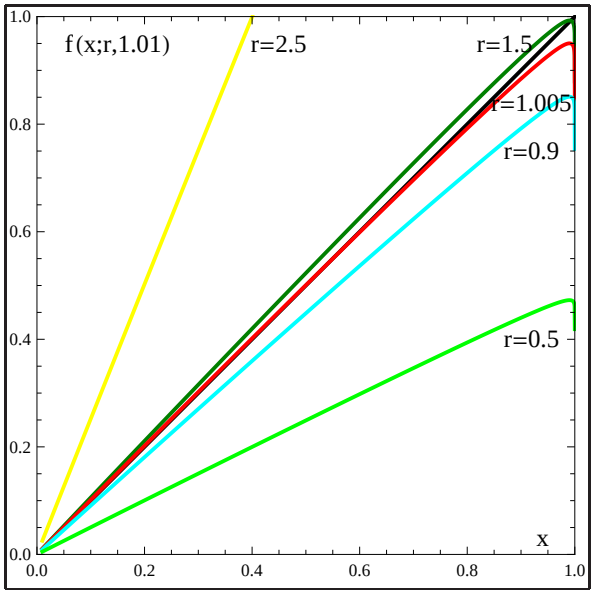

Fig. 4: Graphics of the WGF functions $f(x;r,\alpha)$ at the degenerated case for $\alpha = 1.01$ and $r = 2.5, 1.05, 1.005, 0.9, 0.5$. Remark that some values of the intrinsic growth rates were chosen in order to illustrate the results presented in Table 1.

restricted to R. The fractal "box-within-a-box" structure concerns all types of smooth unimodal maps, with correctly chosen parameter variation.

Nevertheless, an interval of existence of an attractive limit set at a finite distance can be defined by,

$$\bar{\Omega}_1 = [0, r_1^*], \text{ where } r_1^* = \zeta(\alpha), \ \forall r > 0 \text{ and } \forall \alpha > 1, \quad (12)$$

with r_1^* given by Eq.(11). This set is called box $\bar{\Omega}_1$, inside which occurs all the possible bifurcations of the WGF functions. We note that the first real positive bifurcation value is obtained for $r_1^1 = \psi_1(x;\alpha)$, given by Eq.(10), and that the value of fold bifurcation for $n = 1$ is real negative, see Fig.3. Considering the restriction to the parameter region R, the bifurcation curves are limited inferiorly by the flip bifurcation curve Λ_1 and superiorly by the chaotic semi-stability curve Λ_{NA}. However, we can not omit the restrictions caused by (i) of $(A5)$, which are also reflected in definitions given by Eq.(12). Remark that this constraint does not exist for $\alpha \geq 2$, see also [26].

From the above considerations, the bifurcation analysis made (from fold and flip bifurcations curves, Fig.3, and numerical simulations of the bifurcation diagram, Fig.2) and the behavior of the symbolic sequences associated to parameters variation, Table 1 and Remark 3, allow us to formalize the following conjecture:

Conjecture 1. Let $f(x;r,\alpha)$ be the WGF functions, defined by Eq.(3), with $1 < \alpha < 2$, $r > 0$ and satisfying $(A1) - (A5)$, $\Lambda_{(n)_0}$ be the fold bifurcation curves, given by $r = \varphi_n(x;\alpha)$, Eq.(8), and Λ_n be the flip bifurcation curves, given by $r = \psi_n(x;\alpha)$, Eq.(9), with all bifurcation curves relative to a cycle of order $n \in \mathbb{N}$. In the limit case, when $\alpha \to 1^+$, it is verified that the fold bifurcation curves $\Lambda_{(n)_0}$, for $n > 1$, and the flip bifurcation curves Λ_n, for $n \geq 1$, intersect on the bifurcation point $P_{BB} = (\alpha \to 1^+, r \to 1^+)$, following the "box-within-a-box" fractal bifurcations structure in the box Ω_1.

Proposition 1. *Let $f(x;r,\alpha)$ be the WGF functions, defined by Eq.(3), with $\alpha > 1$, $r > 0$ and satisfying $(A1) - (A5)$, $\Lambda_{(n)_0}$ be the fold bifurcation curves, given by $r = \varphi_n(x;\alpha)$, Eq.(8), and Λ_n be the flip bifurcation curves, given by $r = \psi_n(x;\alpha)$, Eq.(9), with all bifurcation curves relative to a cycle of order $n \in \mathbb{N}$. If Conjecture 1 is satisfied, then it is verified that in the limit case, when $\alpha \to 1^+$, the point $P_{BB} = (\alpha \to 1^+, r \to 1^+)$ is a big bang bifurcation point for WGF functions $f(x;r,\alpha)$, from which the fold bifurcation curves $\Lambda_{(n)_0}$, for $n > 1$, the flip bifurcation curves Λ_n, for $n \geq 1$, and the chaotic semi-stability curve Λ_{NA} are issuing, following the "box-within-a-box" fractal bifurcations structure in the box Ω_1.*

Proof. From Eq.(4), the WGF functions $f(x;r,\alpha)$ have one fixed point given by,

$$A_{r,\alpha} = e^{-r^{(1-\alpha)^{-1}}}. \quad (13)$$

If $\alpha \to 1^+$, for each $r > 0$ fixed, it is verified that,

$$\lim_{\alpha \to 1^+} f(x;r,\alpha) = rx. \quad (14)$$

Thus, when $\alpha \to 1^+$ and $r \to 1^+$, from Eqs.(13) and (14) the WGF functions are a degenerated case defined by,

$$f(x; r \to 1^+, \alpha \to 1^+) = x,$$

and the fixed point $A_{r,\alpha}$ converges to $x = 1$. In this limit case, the dynamics cannot escape from the interval $]0,1]$ (besides a hyperbolic set of zero measure), see Fig.4. These conditions are sufficient to state the existence of the big bang bifurcation point $P_{BB} = (\alpha \to 1^+, r \to 1^+)$. Therefore, from Conjecture 1 and Property 1 the desired result follows.

So, in the studied parameters region R we have a big bang bifurcation point P_{BB} with the "box-within-a-box" fractal bifurcations structure, associated to the boxe Ω_1, where an infinite number of bifurcation curves issue from. Now, we are ready to formulate the concept of big bang bifurcation point for the WGF functions, described and characterized on the previous results.

Definition 1. *Let $f(x;r,\alpha)$ be the WGF functions, defined by Eq.(3), with $\alpha > 1$, $r > 0$ and satisfying $(A1) - (A5)$. The point $P_{BB} = (\alpha \to 1^+, r \to 1^+)$ is the big bang bifurcation point of the WGF functions, with a fractal structure of "box-within-a-box" type.*

5 Conclusions and discussion

The present work is an original contribution to the knowledge of the dynamical behavior of the class of WGF's continuous functions, which can be used in the study of tumor growth models. Moreover, we investigated and characterized the bifurcation structure of the WGF functions: the big bang bifurcation point of the so-called "box-within-a-box" type occurs, in the two-dimensional (α, r) parameter space. The existence of this particular type of bifurcation is evidenced through the use of symbolic dynamics techniques and bifurcation theory. However, such as analyzed in Subsec.4.2 and also in paper [26], the presence of big bang bifurcation points is associated with loss of negative Schwarzian derivative.

It is still an open question for which class of maps similar results can be obtained. However, it is well known that the big bang bifurcations occur in the context of piecewise-smooth discontinuous dynamics, whenever two fixed points cross simultaneously the boundary and become virtual, see [3], [4], [5], [8] and references therein. Surely in the sequence of the paper [26], this work is also a new contribution in the big bang bifurcation analysis for continuous maps. It can be expected, that the phenomena of big bang bifurcations for continuous-defined one-dimensional maps is directly related to the derivative, at a fixed point or in its pre-image, not be defined.

Acknowledgment

Research partially sponsored by national funds through the Fundação Nacional para a Ciência e Tecnologia, Portugal-FCT, under the project PEst-OE/MAT/UI0006/ 2014, CEAUL and ISEL.

FCT

Appendix: Symbolic dynamics

Symbolic dynamics is a research topic of discrete dynamical systems which has been widely investigated by Professor Sousa Ramos, by his research group and collaborators. This theory is composed by a set of results, methods and techniques, which have a primordial role in the study of qualitative and quantitative properties of discrete dynamical systems. The topological complexity of a dynamical system is usually measured by its topological entropy. This numerical and topological invariant is associated to the growth rate of the several states of dynamical systems. For more details on these topics see for example [11], [12], [15], [16], [21], [22], [32] and references therein.

Consider for each value of the parameter $r > 0$, the orbit of the critical point $c = e^{1-\alpha}$, with $\alpha > 1$, is given by

$$O_r(c) = \left\{ x_k : x_k = f^k(c; r, \alpha),\ k \in \mathbb{N}_0 \right\} \qquad (15)$$

defined by an iterative process, where

$$x_k = f^k(c; r, \alpha) = f^k(x_{k-1}; r, \alpha).$$

Thus, for each value of the intrinsic growth rate is considered the orbit of the number of cells when the growth rate is maximum. In order to study the topological properties of these orbits, we associate to each orbit $O_r(c)$ a sequence of symbols, corresponding to the critical point itinerary, denoted by $S^{(r)} = S_0^{(r)} S_1^{(r)} S_2^{(r)} \ldots S_k^{(r)} \ldots$, with $k \in \mathbb{N}_0$, where $S_k^{(r)}$ belongs to the alphabet $\mathscr{A} = \{L, C, R\}$, with each symbol defined by

$$S_k^{(r)} = \begin{cases} L \text{ if } f^k(c; r, \alpha) < c \\ C \text{ if } f^k(c; r, \alpha) = c \\ R \text{ if } f^k(c; r, \alpha) > c \end{cases}.$$

Note that the alphabet $\mathscr{A}$ is an ordered set of symbols, corresponding to the intervals of monotonicity and to the critical point of the WGF functions $f(x; r, \alpha)$. The real line order induces naturally an order relation in the alphabet $\mathscr{A}$, so $L \prec C \prec R$. The space of all symbolic sequences of the alphabet $\mathscr{A}$ is denoted by $\mathscr{A}^{\mathbb{N}}$.

The expansive maps admit Markov partitions, whose existence is implicit in the works of Bowen and Ruelle. In this study, we consider the existence of Markov partitions, which are characterized by the orbit of the critical point of the function $f(x; r, \alpha)$, see for example [22]. Consider the set of points corresponding to the k-periodic orbit or kneading sequence of the critical point

$$S^{(r)} = (C S_1^{(r)} S_2^{(r)} \ldots S_{k-1}^{(r)})^{\infty} \in \mathscr{A}^{\mathbb{N}}.$$

This set of points determines the Markov partition of the interval $I = \left[f^2(c; r, \alpha), f(c; r, \alpha) \right]$ in a finite number of subintervals, denoted by $\mathscr{P}_I = \{I_1, I_2, \ldots, I_{k-1}\}$. The dynamics of the WGF functions $f(x; r, \alpha)$ are completely characterized by the symbolic sequence $S^{(r)}$ associated to the critical point itinerary. The WGF functions $f(x; r, \alpha)$ and the Markov partitions associated induce subshifts of finite type whose Markov transition matrices $A = [a_{ij}], (k-1) \times (k-1)$, are defined by

$$a_{ij} = \begin{cases} 1, \text{ if } int\,(I_j) \subseteq f(int\,(I_i); r, \alpha) \\ 0, \text{ otherwise} \end{cases}. \qquad (16)$$

Usually, the subshift is denoted by $(\sum_A, \sigma)$, where σ is a shift map in $\sum_{k-1}^{\mathbb{N}}$ defined by $\sigma(S_1 S_2 \ldots) = S_2 S_3 \ldots$, with $\sum_{k-1} = \{1, \ldots, k-1\}$ corresponding to the $k-1$ subshifts states.

The topological entropy of the WGF functions $f(x;r,\alpha)$, in the phases space, is defined in the associated symbolic space as the asymptotic growth rate of the admissible words (finite symbolic sequences) in relation to the length of the words, i.e.,

$$h_{top}(f) = \lim_{n\to\infty} \frac{\ln N(n)}{n} \tag{17}$$

where $N(n)$ is the number of admissible words of length n. For a subshift of finite type, unidirectional or bidirectional, described by the Markov transition matrix A, the topological entropy is given by $h_{top}(\sigma) = \ln(\lambda_A)$, where λ_A is the spectral radius of the transition matrix A. For a more detailed approach about subshifts of finite type and the Perron-Frobenius Theorem for Markov transition matrix, see [12], [15], [22] and references therein.

References

[1] S.M. Aleixo, J.L. Rocha, J. Comput. Inf. Technol. **20**, 201-207 (2012).
[2] V. Avrutin, G. Wackenhut, M. Schanz, in Proc. Int. Conf. Tools for Mathematical Modelling (Mathtols'99), St. Petersburg, 4-20 (1999).
[3] V. Avrutin, M. Schanz, Nonlinearity **19**, 531-552 (2006).
[4] V. Avrutin, M. Schanz, S. Banerjee, Nonlinearity **19**, 1875-1906 (2006).
[5] V. Avrutin, A. Granados, M. Schanz, Nonlinearity **24**, 2575-2598 (2011).
[6] J-P. Carcasses, Sur Quelques Structures Complexes de Bifurcations de Systemes Dynamiques, Doctorat de L'Universite Paul Sabatier, INSA, Toulouse (1990)
[7] D. Fournier-Prunaret, Int. J. Bifurc. Chaos **1**, 823-838 (1991).
[8] L. Gardini, U. Merlone, F. Tramontana, J. Econ. Behav. Organ. **80**, 153-167 (2011).
[9] F. Kozusko, Z. Bajzer, Math. Biosci. **185**, 153-167 (2003).
[10] A.K. Laird, S.A. Tyler, A.D. Barton, Growth **29**, 233-248 (1965).
[11] J.P. Lampreia, J. Sousa Ramos, Portugaliae Math. **54 (1)**, 1-18 (1997).
[12] D. Lind, B. Marcus, An Introduction to Symbolic Dynamics and Codings, Cambridge University Press, Cambridge, 1995.
[13] A.S. Martinez, R.S. González, C.A.S. Terçariol, Physica A **387**, 5679-5687 (2008).
[14] M. Marušić, Ž. Bajzer, J. Math. Anal. Appl. **179**, 446-462 (1993).
[15] W. Melo, S. van Strien, One-Dimensional Dynamics, Springer, New York, 1993.
[16] J. Milnor, W. Thurston, Dynamical systems (College Park, MD, 1986/87), Lecture Notes in Math., 1342, Springer, Berlin, 465-563, 1988.
[17] C. Mira, Chaotic Dynamics. From the One-Dimensional Endomorphism to the Two-Dimensional Diffeomorphism, World Scientific, Singapore, 1987.
[18] C. Mira, L. Gardini, A. Barugola, J-C Cathala, Chaotic Dynamics in Two-Dimensional Noninvertible Maps, World Scientific Series on Nonlinear, Science Series A, Vol.20., 1996.
[19] M. Misiurewicz, Inst. Hautes Études Sci. Publ. Math. **53**, 17-51 (1981).
[20] D.D. Pestana, S.Velosa, Introdução à Probabilidade e à Estatística, Fundação Calouste Gulbenkian, Lisboa, 2008.
[21] J.L. Rocha, J. Sousa Ramos, J. Difference Equ. Appl. **9**, 319-335 (2003).
[22] J.L. Rocha, J. Sousa Ramos, Int. J. Math. Math. Sci. **38**, 2019-2038 (2004).
[23] J.L. Rocha, D. Fournier-Prunaret, A-K. Taha, Discrete Contin. Dyn. Syst.-Ser.B **18 (9)**, 2397-2425 (2013).
[24] J.L. Rocha, S. Aleixo, Math. Biosci. Eng. **10 (2)**, 379-398 (2013).
[25] J.L. Rocha, S. Aleixo, Discrete Contin. Dyn. Syst.-Ser.B **18 (3)**, 783-795 (2013).
[26] J.L. Rocha, D. Fournier-Prunaret, A-K. Taha, Nonlinear Dyn. **77 (4)**, 1749-1771 (2014).
[27] J.L. Rocha, S. Aleixo, A. Caneco, J. Appl. Nonlinear Dyn. **3 (2)**, 115-130 (2014).
[28] J.L. Rocha, S. Aleixo, A. Caneco, Chaotic Modeling and Simulation, Int. J. Nonlinear Sci. **4**, 519-528 (2013).
[29] S. Sakanoue, Ecol. Model. **205**, 159-168 (2007).
[30] H. Schättler, U. Ledzewicz, B. Cardwell, Math. Biosci. Eng. **8**, 355-369 (2011).
[31] S. Schreiber, J. Math. Biol. **42**, 239-260 (2001).
[32] A.N. Sharkovsky, S.F. Kolyada, A.G. Sivak, V.V. Fedorenko, Dynamics of One-Dimensional Maps, Kluwer Academic Publishers, Netherlands, 1997.
[33] D. Singer, SIAM J. Appl. Math. **35**, 260-267 (1978).
[34] M. Turner, E. Bradley, K. Kirk, K. Pruitt, Math. Biosci. **29**, 367-373 (1976).
[35] M. Turner, K. Pruitt, Math. Biosci. **39**, 113-123 (1978).
[36] A. Tsoularis, Res. Lett. Inf. Math. Sci. **2**, 23-46 (2001).
[37] P. Waliszewski, J. Control Eng. and Appl. Informatics **4**, 45-52 (2009).

J. Leonel Rocha received his Diploma in 1994, the Masters degree in 1998 and the Ph.D. degree in 2004, all in Mathematics, the last ones were obtained from the Technical University of Lisbon, School of Engineering (IST). Currently, he is Coordinator Professor at the Department of Mathematics of the Superior Institute of Engineering of Lisbon (ISEL). Since 1997, his research has been centered on dynamical systems: discontinuous maps, symbolic dynamics, topological and metrical invariants. He continued research in Applied Mathematics at the Center of Statistics and Applications of the University of Lisbon (CEAUL). His interests are in the areas of population dynamics, bifurcation theory, networks, synchronization and applications.

A. K. Taha received a Masters degree in pure mathematics (1984) and two doctorates in applied mathematics (1987 and 1989), at INSA Toulouse, France. Currently, he is Professor of Mathematics at the department of computer science at the Technology Institute of the University of Toulouse and researcher at the Department of Electrical Engineering and Computer Science at INSA. His interests are in continuous and discontinuous dynamical systems (especially bifurcation theory, mappings with double indices and population dynamics), special function theory, arithmetic and history of mathematics.

D. Fournier-Prunaret obtained a Ph.D. degree in Nonlinear Dynamical Systems, then a Doctorat d'Etat at the University Paul Sabatier of Toulouse, France, respectively in 1981 and 1987. She is currently Professor at the National Institute of Applied Sciences (INSA) in Toulouse, France. She has been the Head of the LATTIS (Toulouse Laboratory of Technology and System Engineering) from 2006 to 2010 and she is now the Director for International Relations at INSA. Her research and teaching activities concern Modelisation and Analysis of Nonlinear Dynamical Systems, focusing more particularly on the study of Chaos and Applications to Telecommunications, Secure Transmissions and Biology. She is the author of more than 100 papers in international journals and conferences related to the study of Nonlinear Maps.